Photoionization of isoelectronic ions: Mg^+ and Al^{2+}

A. Aguilar,[1,2] J. B. West,[3] R. A. Phaneuf,[1] R. L. Brooks,[4] F. Folkmann,[5] H. Kjeldsen,[5] J. D. Bozek,[2] A. S. Schlachter,[2] and C. Cisneros[6]

[1]*Department of Physics, MS220, University of Nevada, Reno, Nevada 89557*
[2]*Advanced Light Source, Ernest Orlando Lawrence Berkeley National Laboratory, University of California, Berkeley, California 94720*
[3]*CLRC Daresbury Laboratory, Warrington WA4 4AD, United Kingdom*
[4]*Guelph-Waterloo Physics Institute, University of Guelph, Ontario, Canada N1G 2W1*
[5]*Institute of Physics and Astronomy, University of Aarhus, DK-8000 Aarhus C, Denmark*
[6]*Centro de Ciencias Físicas, Universidad Nacional Autónoma de México, Apartado Postal 6-96, Cuernavaca 62131, Mexico*

High-resolution measurements of the photoionization cross sections of the Na-isoelectronic ions Mg^+ and Al^{2+} are presented, to be compared with earlier measurements in which structure in the most prominent peaks was unresolved. These measurements have been normalized to the earlier ones in order to provide values of the oscillator strengths of the newly resolved peaks, and comparison is made with multiconfiguration Hartree-Fock calculations.

I. INTRODUCTION

The ready availability of access to synchrotron radiation from undulators on electron storage rings has led to a marked increase in experimental data on photoionization of atomic ions, and in particular on absolute measurements. This has made it possible to carry out long awaited checks on theoretical data from major computational programs such as the OPACITY [1] and IRON [2] projects. Both the limitations and successes of those calculations have come to light, as can be seen in a recent review on this topic [3]. Such comparisons with theoretical calculations make a fundamental contribution to our understanding of basic atomic physics, probed by the photoionization process. The measurements are also relevant to the modeling of both stellar atmospheres, bearing in mind that the vast majority of matter in the universe is in ionic form, and laboratory plasmas.

Although the first absolute measurements were made some time ago [4], using the merged beam technique, they were limited to cross sections $\gtrsim 10$ Mb since they were carried out on a bending magnet source having limited photon flux. An undulator source, besides being much more intense, also has the advantage that the radiation is well collimated both vertically and horizontally, and is therefore ideally matched to the merged beam type of experiment. This method has now become a standard in synchrotron-radiation laboratories in Japan at the Photon Factory and Spring-8, in France at Super-ACO, in the USA at the Advanced Light Source, and in Denmark on the storage ring ASTRID.

It is instructive to study both isonuclear and isoelectronic sequences, to observe the evolution of spectral structure and cross sections. To date, the majority of such experiments have been carried out using laser plasma sources [5], which have good access to highly charged states; an example of a very different behavior that can be observed is the Ar isoelectronic sequence of ions [6]. Recently, however, electron cyclotron resonance (ECR) sources have been used with the merged beam method for measurements on the multiply charged ions of Xe, Ba, and C [7–9]. This kind of ion source is not always well suited to absolute measurements since, owing to the high energy of the electrons in the plasma, the parent ion beam may well contain a large fraction of metastable states, but it does give access to highly charged ions. The experiment undertaken here makes use of an ECR source, but relies for the absolute values of the cross section on measurements made earlier with a low-energy discharge ion source. The earlier measurements [10] were carried out on a beam line with substantially lower resolving power, and although absolute, much of the structure could not be resolved and thereby identified with certainty; comparison with theoretical calculations was therefore not definitive. This experiment demonstrates the complementarity of the two experiments, the earlier one providing the absolute basis for the measurements, to which the results of the experiment presented here could be normalized, thereby providing absolute measurements with state-of-the-art spectral resolution.

II. EXPERIMENTAL METHOD

The experimental work was carried out on beam line 10.0.1 at the Advanced Light Source at the Lawrence Berkeley National Laboratory. This is an undulator beam line fitted with a spherical grating monochromator covering the photon energy range 17–340 eV. Typical photon fluxes at a photon energy of 65 eV were between 2×10^{12} and 4×10^{13} photons/sec for bandpasses in the range 6–60 meV; further details of the specification and performance of this beam line are to be found in Refs. [12] and [13]. The exit beam from the monochromator and its postfocusing optics were merged with the ion beam over a length of 29 cm [14]; the ions were generated in an ECR source containing a resistively heated oven to vaporize the metal samples.

Although the experimental equipment contained the beam scanners and calibrated detectors required to make absolute measurements, as pointed out earlier this was unnecessary for the measurements presented here, where the emphasis was on spectral resolution. Given the weakness of the parent ion beam—typical currents for Al^{2+} were in the range 1–10

nA—each spectrum consisted of several overlapping scans with a dwell time of 2 sec/point, to minimize the effects of drift in the ion-beam or photon-beam overlap. A chopper in the photon beam enabled measurements of the background in the ionization signal channel to be measured, and for the data shown here this background has been subtracted. As seen in some of the spectra shown, this can result in a negative signal where the signal was low and dominated by statistical fluctuations. The data were corrected for varying ion currents and incident photon intensities.

III. THEORETICAL CALCULATIONS

Calculations were performed using the atomic structure package of Froese Fischer *et al.* [15] in a manner similar to that described previously [10]. The large number of energetically, closely spaced, interacting states calls for a configuration-interaction (CI) type of calculation. The wave functions were obtained using the multiconfigured version of the program (MCHF) in steps. The $1s$, $2s$, $2p$, and $3p$ orbitals were obtained by calculating the $1s^2 2s^2 2p^5 3p^2$ ^2P term, multiconfigured, and then keeping these orbitals fixed for subsequent steps. The $3s$ and $3d$ orbitals were obtained by calculating the $1s^2 2s^2 2p^5 3s 3d$ ^2P term, also multiconfigured, but with only the $3s$ and $3d$ orbitals varying. The $4s$, $4p$, $4d$, $5s$, $5d$, and $6d$ orbitals were likewise obtained in six steps with only those orbitals varying in each step. The ^2P terms were used throughout as being representative of the configuration average, but only for the purpose of obtaining the wave functions.

Once the wave functions were obtained, a CI calculation was also performed in steps. Only those odd-parity energy levels that have dipole allowed transitions from the ground state were considered. *LS* coupling was used, though it is not "good," so all odd-parity terms having levels with $j = 3/2$ or $1/2$ were considered. We eventually dropped ^4P terms, finding that their levels had vanishingly small f values. Starting with the lower-lying configurations, we considered all levels from the ^2S, ^2P, and $^{2,4}D$ terms. The $2p^5$ subshell was coupled last, so the configurations considered were the $3s^2 2p^5$, $3p^2 2p^5$, $4p^2 2p^5$, and the $3s n\ell 2p^5$, with $n\ell$ being $4s$, $3d$, $4d$, and $5s$, $5d$, and $6d$. In total, 52 energy levels were considered for Mg$^+$ but program limitations prevented us from doing them all together. By dividing the problem into manifolds by energy region, we were able to keep track of which terms were interacting the most, and assigned *LS* term designations based on the predominant term for each level considered.

When doing CI calculations such as these, the isoelectronic nature of Mg$^+$ and Al^{2+} is not so useful and the ions were treated individually with respect to level interactions and the decisions taken for term designations. Even the stepwise process for performing the calculations was somewhat different for the two ions, more as a consequence of the calculations being performed at different times on different computers than for any substantive reason. The description given previously was for Mg$^+$, but a very similar procedure was followed for Al^{2+}.

Finally, a comment on the energy shift needed to compare
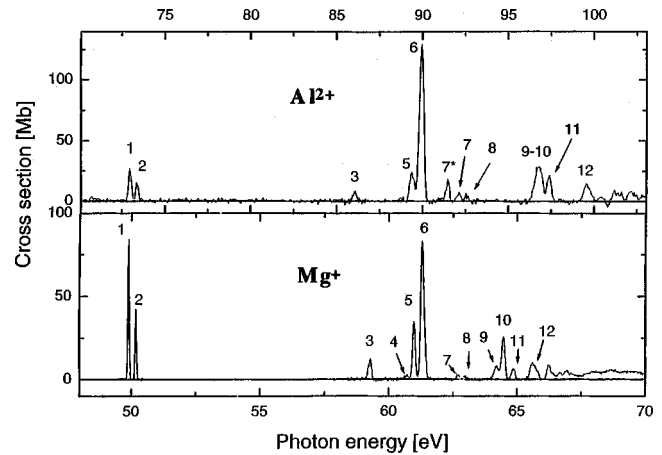
FIG. 1. The photoionization spectrum of Mg$^+$ and Al^{2+}, taken from Ref. [10].

to the experimental values seems appropriate. Because the ground state of both ions has a complete $n = 2$ shell while all of the excited states in these experiments have a promoted $2p$ electron, the $2p$ orbitals for the ground state and excited states would be quite different. The amount of multiconfiguring needed for the ground state and excited states to account for correlation would also be quite different, and while it is straightforward to extensively multiconfigure the ground state, it is not straightforward (and maybe not even useful) to extensively multiconfigure the orbitals for a CI calculation. Because of this, the correlation offset between the ground state and *all* of the excited states is different, and we have evaluated that difference to be 1.0 eV for Mg$^+$. We have chosen not to correct the tabulated numbers accordingly, but this error is not indicative of the relative placement of the excited-state energy levels themselves.

IV. EXPERIMENTAL RESULTS

A. Mg$^+$

In order to guide the reader, we have reproduced in Fig. 1 the figure for the spectra of Mg$^+$ and Al^{2+}, from the previous paper [10] on these two ions. This gives the numbering scheme which was used to identify the various peaks observed and which is used frequently in this paper.

We focus first on peaks 3, 5, and 6 between 59 and 61.5 eV, for which the data are shown in Table I. The peak at 61.3 eV is the most prominent in the spectrum and was the one whose assignment was a major point of discussion in the earlier papers [11,10]. Given the scatter in the data points, it seemed a reasonable simplification to use a Gaussian profile for the spectral lines, so the continuous lines seen in the figures are Gaussian fits to the data. It was assumed that the peak width would be the same for all the peaks, but this width was allowed to vary during the fitting process. In all the figures and text below, the spectral resolution given is the full width at half maximum (FWHM) obtained from the fitting process, rather than the nominal value obtained from the monochromator exit slit setting; also, any contribution from the natural linewidth has been ignored. These fits were used

TABLE I. Identities and parameters of the lines observed in Mg$^+$ between 59 and 61.5 eV.

Line [b]	Energy (eV)		Identity		Oscillator strength [a]	
	Expt.	Calc.	West *et al.* [10]	This work [c]	This expt.	Calc.
3a	59.21	58.23	$(3p^2\,^1D+3s3d\,^1D)\,^2P_{1/2}$	$(3p^2\,^1D+3s3d\,^1D)\,^2P_{1/2}$	0.005	0.027
3b	59.3	58.32	$(3p^2\,^1D+3s3d\,^1D)\,^2P_{3/2}$	$(3p^2\,^1D+3s3d\,^1D)\,^2P_{3/2}$	0.01	0.049
4 [d]	60.71[d]	59.61	$(3p^2\,^3P)\,^2P$	$(3p^2\,^3P)\,^4D$ [e]		0
5	60.95	59.96	$(3s3d\,^3D)\,^4D,\ (3s4s\,^3S)\,^2P$	$(3s3d\,^3D)\,^4D$	0.009	0.048
	60.98	60.02		$(3s4s\,^3S)\,^2P$	0.021	0.065
	61.0	60.12		$(3p^2\,^3P)\,^2S$	0.01	0
6	61.30	60.29	$(3s3d\,^3D)\,^2P,\,^2D$	$(3s3d\,^3D)\,^2P_{3/2}$	0.076	0.203
	61.37	60.39		$(3s3d\,^3D)\,^2P_{1/2}$	0.032	0.140
	61.41	60.4		$(3s3d\,^3D)\,^2D$	0.07	0.081
	61.43	60.45		$(3s4s\,^1S)\,^2P_{3/2}$	0.07	0.008

[a]Experimental values are $\pm 20\%$.
[b]Numbering taken from Refs. [11,10].
[c]Assignment for most prominent configuration.
[d]Not observed in this experiment.
[e]From current theoretical calculation.

in partitioning the oscillator strength following normalization to the earlier absolute measurements; an error of $\pm 20\%$ is estimated for the values given in the tables. Varying resolutions were used for the spectra taken; use of the highest resolution of 7 meV was limited to the case where the cross section was highest, as in the $3p \rightarrow 3d$ region of Mg$^+$ shown in Fig. 4. Elsewhere, a compromise between the count rate and resolution was necessary to obtain spectra in a reasonable time period.

The data for peak 3 are shown in Fig. 2, where there is a spin-orbit doublet $^2P_{3/2,1/2}$ associated with the strongly mixed $3p^2\,^1D$ and $3s3d\,^1D$ configurations; this doublet is now clearly resolved at the 18-meV resolution (FWHM) of the current experiment. The ratio of the peak areas is 2.05:1, which is distinct from 1.7:1 found in the earlier work; but otherwise the results from the two experiments are identical. We note that peak 4 was not observed in the current work. The reason for this is not clear, but it was a weak feature and

the narrow bandpass of this experiment would make it more difficult to observe. Peak 5 is now seen to be three peaks, as shown in Fig. 3, where the spectral resolution was 11 meV.

The spectrum in the region of peak 6 is shown in Fig. 4, where with a bandwidth of 7 meV, four lines are now clearly seen in this region. The peak positions and oscillator strengths normalized to the earlier absolute measurements are shown in Table I, together with the previous assignments and those made in the present work based on MCHF calculations. The calculated energies should be shifted upwards by ~ 1 eV; the value of this shift is taken from the experimental and theoretical values for the position of the $2p^5 3s^2\,^2P_{1/2,3/2}$ doublet, which was well resolved in the early experiment [11] and for which the identity and energies are well known. Using this shift, and the relative calculated values of the oscillator strengths compared to the experimental ones—the theory obviously overestimates the absolute values—it was possible to assign the newly resolved levels as shown in the table.
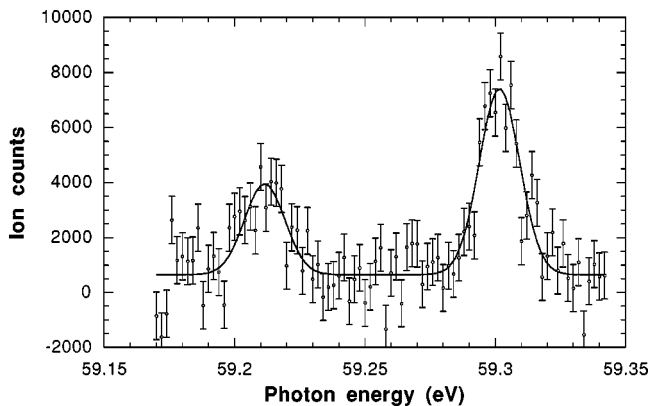
FIG. 2. The photoionization spectrum of Mg$^+$ in the region of peak 3; the experimental resolution was 18 meV.
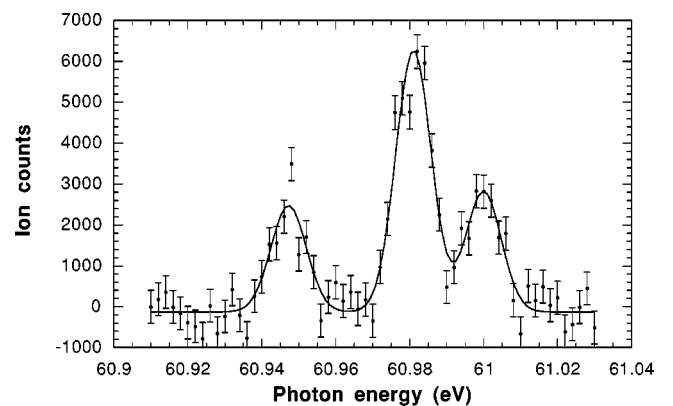
FIG. 3. The photoionization spectrum of Mg$^+$ in the region of peak 5; the experimental resolution was 11 meV.
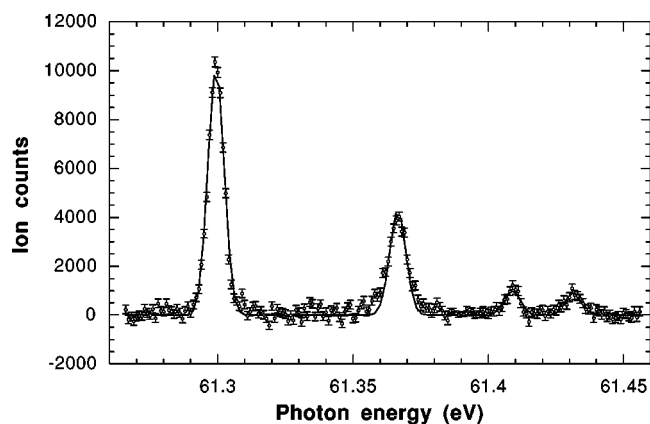
FIG. 4. The photoionization spectrum of Mg^+ in the region of peak 6; the experimental resolution was 7 meV.

There are still ambiguities: the weak lines at 61.41 and 61.43 eV could both be assigned to the $(3s4s\ ^1S)\ ^2P_{3/2,1/2}$ doublet, but the theoretical value for the splitting is 0.20 eV, so the energies would not match the experimental ones as well, after accounting for the 1-eV shift. In this instance the relative calculated values of the oscillator strengths do not help; both indicate an order of magnitude of difference in the relative oscillator strengths, in clear contradiction with experiment if the assignments shown are correct.

Even though the current experiment has a similar resolution to that of Esteva and Mehlman [16], comparison with the earlier experiment (where the target species was produced in a discharge) and their later revised assignments [17] does not produce any new information. The weak lines at 61.41 and 61.43 eV were not observed in the earlier experiment, but lines at 61.09 and 61.22 eV were in contrast to the more recent experiments [10,11], including this one. The major difference was that Mehlman *et al.* [17] assigned the lines at 61.30 and 61.38 eV to $(3s4s\ ^1S)\ ^2P_{3/2,1/2}$ transitions [17], whereas these were originally reassigned to a mixture of $(3s3d\ ^3D)\ ^2P,\ ^2D$ transitions [10]. The basis for this reassignment was that, in principle, $3s3d$ transitions were expected to be much stronger than $3s4s$ transitions. Configuration mixing makes the situation far more complex, but the MCHF calculations supported this; also, absolute values of the oscillator strengths were available to assist in the analysis. The current measurements support the more recent analysis and the newly resolved structure matches the MCHF calculations quite well, apart from the absolute values of the oscillator strengths. It was also possible to extend the analysis by proposing individual assignments for the fine structure resolved in the current work, as seen in Table I.

The region between 64 and 68 eV is shown in Fig. 5, where peaks were seen previously [11] but not resolved. The Gaussian fits are not shown for this figure, but were used in calculating the oscillator strengths as before in those regions where the structure was not clearly resolved or scatter in the data prevented the peaks concerned from being clearly defined. This was particularly the case for the doublet in the region of 66.25 eV, and the peaks between 66.9 and 67.5 eV. The two prominent features at $\sim$64.5 and 65.7 eV are seen to contain several lines. The analysis, summarized in Table II,
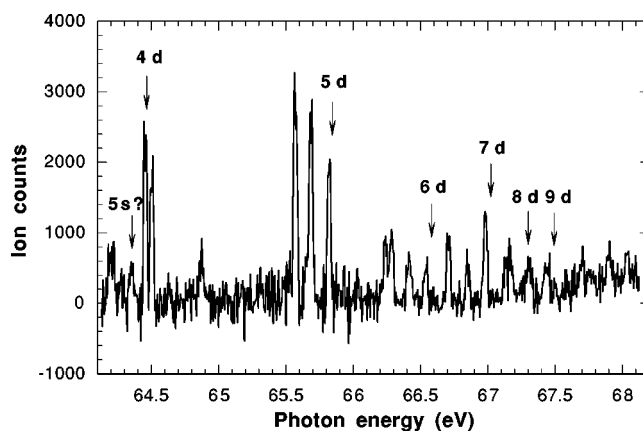
FIG. 5. The photoionization spectrum of Mg^+ in the region between 64 and 68 eV; the experimental resolution was 30 meV. The arrows indicate the positions of lines calculated from a Rydberg analysis.

is based on both the MCHF calculations and also on a simple Rydberg calculation for an nd series, based on the line at 61.3 eV being $3s3d$ and that at 64.46 being $3s4d$; a quantum defect of 0.19 was determined, consistent with a d series. This analysis gave some idea of where the prominent configurations might lie and are indicated by arrows in the figure; the results are also shown in the table. The experimental oscillator strengths shown have been calculated by normalization to the earlier experiment.

The MCHF calculation predicts that there will be strong interaction between the $3p^2\ ^1S$ and $3s4d$ configurations, and for that reason it is impossible to be certain of the individual assignments in the region around 64.5 eV. The prominent configurations are $(3s4d\ ^3D)\ ^4D$, $(3p^2\ ^1S)\ ^2P$, and $(3s4d\ ^1D)\ ^2D,^2P$, and since the fine structure in these configurations is not resolved, even at the much enhanced resolution of the present experiment, the assignments are speculative. Even so, we have made the assignments based on relative values of the calculated oscillator strengths, as before. There is no good match to line 11 at 64.88 eV, seen in both this and the previous experiment, probably as a result of configuration interaction shifting this line by a greater amount than predicted by theory. The possibility arises that it could be due to a $3s5s$ configuration, but our MCHF calculation indicates that the ns transitions should have negligible oscillator strengths. We return to this point below when discussing the Rydberg analysis of a possible ns series.

The second group of peaks at $\sim$65.7 eV was rather easier to assign, since they are not so strongly perturbed and match the theoretical calculations quite well; they are based primarily on $(3s5d\ ^{1,3}D)$ configurations. Above that, again the assignments become somewhat speculative; it would be possible to assign the triplet of lines at 66.24, 66.29, and 66.42 eV to the calculated $3s6d$ configurations at 65.19, 65.28, and 65.37 eV, in a way similar to the $3s5d$ lines, but it is not clear that this would give the best alignment of the experimental energies with the theoretical values. In Table II, therefore, the lines have been listed in their energy order. Based on the present calculation, it is difficult to be definitive on the individual assignments of each line, but it seems clear

TABLE II. Identities, parameters, and effective principal quantum numbers (n^*) of the lines observed in Mg$^+$ between 64 and 68 eV.

Line	Energy		Identity		Oscillator strength		n^*	Energy (eV)
	Expt.	Calc.	West et al. [10]	This work	Expt.	Calc.		
9	64.21	63.28	$3s\,^3P_2\,4d_{3/2}$ $+3s\,^3P_2\,5s_{1/2}$ $+3s\,^3P_1\,4d_{3/2,5/2}$	$(3p^2\,^1S)\,^2P_{3/2}$	0.013	0.005		
10	64.46	63.4	$3s\,^3P_1\,5s_{1/2}$	$(3s4d\,^3D)\,^4D$	0.023[a]	0.004	3.81 [b]	64.46
	64.51	63.52	$+3s\,^3P_0\,4d_{3/2}$	$(3p^2\,^1S)\,^2P_{1/2}$	0.018[a]	0.007		
		63.63	$+3s\,^3P_0\,5s_{1/2}$	$(3s4d\,^1D)\,^2D$		0.006		
		63.67	$+3s\,^3P_2\,4d_{5/2}$	$(3s4d\,^1D)\,^2P$		0.005		
11	64.88	63.69	$3s\,^1P_1\,5s_{1/2}$ $+3s\,^1P_1\,4d_{3/2,5/2}$	$(3s4d\,^3D)\,^2P$	0.009	0.014		
12	65.57	64.53	Sum of $3s6s$ and $3s5d$ lines	$(3s5d\,^3D)\,^4D$	0.032	0.007	4.81	65.83
	65.70	64.64		$(3s5d\,^1D)\,^2P$	0.034	0.004		
	65.83	64.74		$(3s5d\,^3D)\,^2D$	0.021	0.009		
13[c]	66.24						5.81	66.55
	66.29	65.19		$(3s6d\,^3D)\,^4D$	0.01	0.002		
	66.42	65.26		$(3s6d\,^1D)\,^2D$	0.011	0.001		
	66.55	65.28		$(3s6d\,^1D)\,^2P_{1/2}$	0.008	0.001		
	66.72	65.37		$(3s6d\,^3D)\,^2D$	0.006	0.005		
		65.81		$(3s6d\,^3D)\,^2P$ $+(3s6d\,^1D)\,^2P_{3/2}$	0.01	0.002		
		66.99			0.02		6.81	67.02
		67.32			0.011		7.81	67.30
		67.45			0.011		8.81	67.49
	Series limit						∞	68.2 [d]

[a]These values refer to the two lines observed at 64.46 eV and 64.51 eV in this experiment.
[b]This assumes that the line at 64.46 eV is the $4d$ member of the Rydberg series.
[c]Observed by Kjeldsen et al. [11], but not numbered by them.
[d]Calculated value.

that this group of lines belongs to configurations of the type $(3s6d\ ^{1,3}D)$. At higher energies, no positive assignments can be made, although higher nd transitions are likely to be the most prominent. The series limit calculated from the Rydberg series analysis is at ~68.2 eV.

An attempt was also made to calculate the positions of the ns series, using the position of the well-established $2p^5 3s^2\ ^2P_{3/2}$ line at 49.90 eV [11,16] and the $3s4s$ line that is part of the line at 60.98 eV (see Table I). A quantum defect of 1.28 was obtained in this way, consistent with an s series, and the positions of the higher series members did coincide with lines in the experimental spectrum; also the series limit was calculated to be at 68.3 eV, in fair agreement with that for the nd series. However, in general, the calculated positions of the ns series overlapped with lines already assigned to nd configurations. The only exception was the line at 64.27 eV, calculated by the Rydberg analysis to be at 64.36 eV and therefore possibly $3s5s$; the MCHF calculations puts the $(3s5s\ ^3S)\ ^2P_{3/2}$ line at 63.60 eV, somewhat closer than the 1-eV discrepancy expected. In view of this, the facts that the ns series is expected to be very weak and the large de-

gree of configuration interaction in the spectrum attempts to confirm the presence of an ns series, were inconclusive.

B. Al^{2+}

The ion-beam intensity for Al^{2+} was generally in the 1–10 nA range and did not remain stable for periods of more than a few hours, thereby limiting the statistical accuracy obtainable in the experiment. We therefore focused on the strongest peaks in the spectrum observed previously [10], numbered 5–12 originally; the summary of our results and assignments and a comparison with the previous data are given in Table III.

The strongest of the lines is peak 6 situated at 89.89 eV, and is shown in Fig. 6. These data were taken at a resolution of 40 meV, and it is clearly seen that at this resolution peak 6 has two components. From the data in the main part of Fig. 6, it is not obvious that there is also a peak at 89.27 eV, which was designated peak 5 [10]. The inset shows the result of the sum of 15 scans through a narrower energy region, indicating that we also see this peak. The main spectrum was

TABLE III. Identities and parameters of the lines observed in Al^{2+}.

Line	Energy (eV) Expt.	Calc.	Identity West *et al.* [10]	This work	Oscillator strength This expt.	Calc.
5	89.29	88.63	$(3s3d\ ^3D)\ ^4D$	$(3s3d\ ^3D)\ ^4D$	0.053[a]	0.071
6	89.72	88.95		$(3p^2\ ^3P_2)\ ^2P_{3/2}$	0.081	0.097
	89.88	89.06	$(3s3d\ ^3D)\ ^2D,\ ^2P$	$(3s3d\ ^3D)\ ^2P_{3/2}$	0.164	0.205
	89.90	89.19		$(3s3d\ ^3D)\ ^2P_{1/2},^2D$	0.132	0.421
7*	91.39	90.65	$(3s4s\ ^3S)\ ^2P$	$(3s4s\ ^3S)\ ^2P_{1/2}$	0.051	0.022
7	92.18	91.29	$(3p^2\ ^1S)\ ^2P_{3/2}$	$(3s4s\ ^1S)\ ^2P_{3/2}$	0.011	0.001
8[b]		91.69	$(3p^2\ ^1S)\ ^2P_{1/2}$	$(3s4s\ ^1S)\ ^2P_{1/2}$		0
9	96.67	95.74		$(3s4d\ ^3D)\ ^4D$	0.063	0.034
10	96.87	96.30	$(3s\ ^3P_{0,1,2})\ 4d[5/2,3/2]$	$(3s4d\ ^{1,3}D)\ ^2P_{1/2,3/2}{}^c$	0.081	0.462
11	97.50	96.55		$(3s4d\ ^{3,1}D)\ ^2P_{1/2,3/2}{}^d$	0.059	0.044
12	99.53[e]		$(3s\ ^3P_{0,1,2})\ 5d[5/2,3/2]$		0.093[e]	

[a]To be compared with 0.068 from Ref. [10]; see text.
[b]Not observed in this experiment, but see text.
[c]$(3s4d\ ^1D)\ ^2P_{1/2}\ +\ (3s4d\ ^3D)\ ^2P_{3/2}$.
[d]$(3s4d\ ^3D)\ ^2P_{1/2}\ +\ (3s4d\ ^1D)\ ^2P_{3/2}$.
[e]To be compared with 99.55 eV and 0.061 from Ref. [10]; see text.

the result of three scans, so it was possible to estimate the oscillator strength of peak 5 by normalization to peak 6. This gives approximate agreement with the previous result for peak 5 (see Table III), although the present result is less reliable, $\sim\ \pm 50\%$, because the two experimental runs were separated by several hours. Consequently, drifts in the overlap integral for the ion and photon beams could render the comparison between two different runs in this way prone to error.

The region near peak 6 was scanned at higher resolution (11 meV), and the results are shown in Fig. 7. Now it is clear that peak 6 actually has three components, with a spin-orbit doublet at 89.88 and 89.90 eV. If we assume an energy difference between theory and experiment of 0.82 eV for the lower member of the doublet, according to our MCHF calculation this member could be assigned to the $(3s3d\ ^3D)$ $^2P_{3/2}$ configuration. The theoretical value of the splitting is then wrong by an order of magnitude, but the high oscillator strengths calculated here support this assignment. The calculation also gives significant oscillator strength to the nearby ^2D configuration, which would not be resolved in our experiment. The third component at lower energy would then be $(3p^2\ ^3P_2)\ ^2P$.

The next region, between 91.2 and 92.6, is shown in Fig. 8, taken with a resolution of 58 meV. Peak 8, originally seen at 92.52 eV with an oscillator strength of 0.014, was not observed. Since this has an oscillator strength five times smaller than that of peak 5, which with the resolution of the present experiment was very difficult to observe, it was not considered worthwhile to devote substantial time to further

FIG. 6. The photoionization spectrum of Al^{2+} in the region between 89.1 and 90 eV; the experimental resolution was 40 meV. The inset shows the peak at 89.27 eV, where the data were taken over a much longer period (see text).
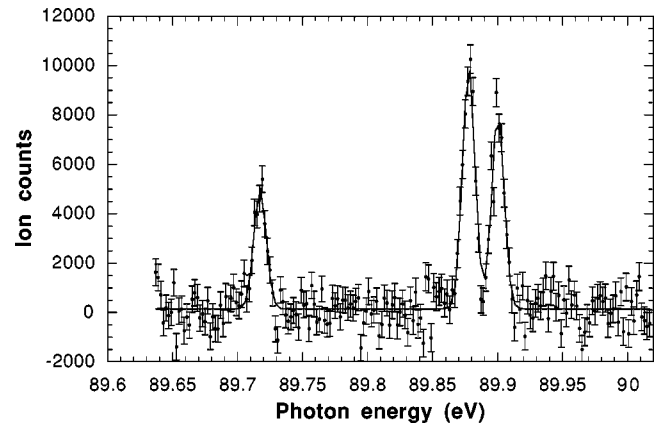
FIG. 7. The photoionization spectrum of Al^{2+} in the region between 89.6 and 90 eV; the experimental resolution was 11 meV.
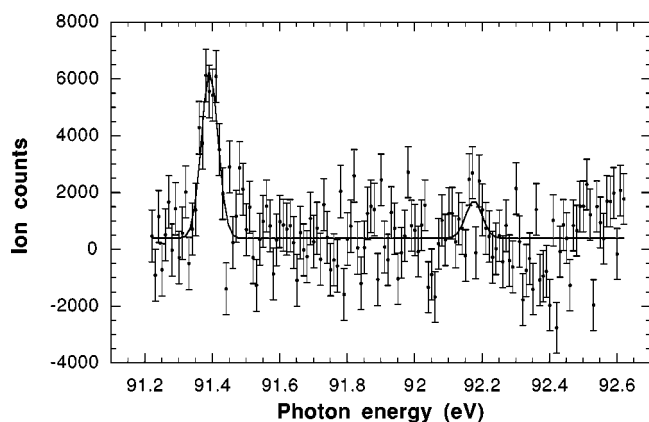
FIG. 8. The photoionization spectrum of Al^{2+} in the region between 91.2 and 91.6 eV; the experimental resolution was 58 meV.

measurements on peak 8. The two peaks seen in Fig. 8 have been identified with peaks 7* and 7, as numbered in the previous work; although possibly as a result of the improved resolution available to the current experiment peak 7 has a slightly different energy of 92.18 eV compared with 92.06 eV originally. To some extent this depends on the reliability of our Gaussian fit; the scatter in the data would not give much confidence in the position we found for this peak, but we found that the fitting process would always converge to the same position even though the estimate was moved by as much as ± 0.2 eV. Whereas the assignment for peak 7* is unchanged, there is now confusion in the assignments for peaks 7 and 8, compared to the previous work. Given their low oscillator strengths and the correlation with the calculated energies, these peaks could more reasonably be assigned to the $(3s4s\ {}^1S)\ {}^2P$ doublet rather than the $(3p^2\ {}^1S)$ ${}^2P$ thought originally. We assume, even though we do not observe it, that peak 8 exists with an oscillator strength rather less than peak 7, noting that in the previous work they were found to have comparable oscillator strengths. This difference between the two experiments may arise because the two peaks were only barely resolved in the previous work.

Figure 9 shows our data for peaks 9, 10, and 11 in the 96.4–97.4 eV photon energy region, where again there are slight energy differences from the earlier data, again prob-
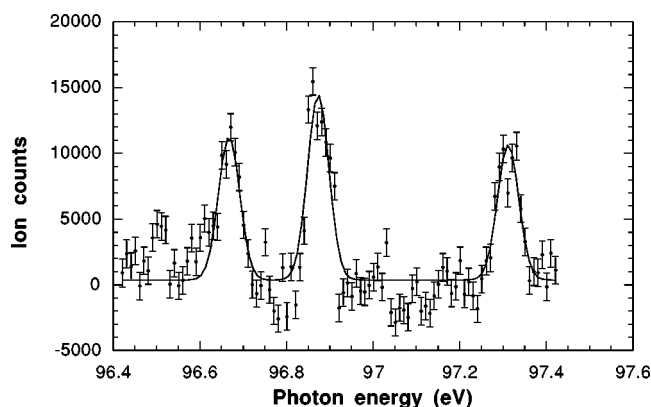
FIG. 9. The photoionization spectrum of Al^{2+} in the region between 96.4 and 97.4 eV; the experimental resolution was 58 meV.

ably due to the different resolutions used in the two experiments. No additional structure was seen in this region compared to the previous work, although the peaks are now quite clearly resolved with our 58-meV resolution. The detailed assignment of these lines is not clear, because the experimental energies do not correlate well with the calculated ones; comparison with the structure and assignments given by Brilly *et al.* [18] does not help, because the energies of the lines we have measured do not coincide accurately with theirs, and they do not provide any intensity information. Even so, it is clear that these lines are to be associated with configurations based on $3s4d$ transitions, as found in the previous work. As above, our assignment has taken into account the theoretical values of the oscillator strengths when choosing the most likely configurations.

Peak 12 was also observed in the present experiment, at a slightly different energy; 28 successive scans were necessary to see this peak clearly. The value of its oscillator strength estimated from this experiment, given the uncertainty in our normalization procedure where different experimental runs were involved as outlined earlier, is likely to be less reliable than the earlier value from Ref. [10].

V. CONCLUSIONS

The order-of-magnitude improvement in resolution in the results of this experiment in comparison to the earlier work [11,10] has permitted us to make more definitive assignments of the most prominent spectral peaks. These peaks were found to contain many more structures than observed originally, most of which were identifiable by means of our MCHF calculations. Also, the general behavior of the oscillator strengths, in terms of relative intensities, is (to some extent) borne out by the experiment, but agreement with the absolute values obtained by the experiment is rather poor. This is largely due to the strong mixing among different configurations, particularly in the region of the $4d$ excitations in Mg$^+$, which are strongly perturbed by the $3p^2\ {}^1S_0$ configuration. This particular perturbation is less obvious in the case of Al^{2+}, and in fact, as seen in Table III, we have changed this assignment compared to the earlier work. It can also be seen that in general the agreement between experiment and theory in the case of the oscillator strengths is somewhat better for Al^{2+} than for Mg$^+$. This indicates that configuration interaction is less prominent in Al^{2+}; simplistically, this would be expected since the orbitals will be better localized in the field of the doubly charged ion.

The most reliable part of the MCHF calculation is in determining the energies of the various configurations; the actual assignments are somewhat arbitrary because in most cases the levels are strongly mixed. The degree of this mixing influences the calculated value of the oscillator strength; and this is the least satisfactory aspect of the present calculation, largely because of its sensitivity to the relative positions of the interacting configurations and the precise form of the wave functions, particularly for the d orbitals. Now that much of the underlying structure has been resolved, it may be worthwhile to attempt more refined calculations to improve this. Even within the limited abilities of the present

calculation, however, it has proved possible to identify most of the clearly resolved features in the experiment, giving a much better understanding of the complex spectra of these two isoelectronic ions.

[1] M.J. Seaton, J. Phys. B **20**, 6409 (1987).

[2] S.N. Nahar and A.K. Pradhan, Phys. Rev. A **49**, 1816 (1994).

[3] J.B. West, J. Phys. B **34**, R45 (2001).

[4] I.C. Lyon, B. Peart, J.B. West, and K. Dolder, J. Phys. B **19**, 4137 (1986).

[5] P.K. Carroll and J.T. Costello, Phys. Rev. Lett. **57**, 1581 (1986).

[6] P. van Kampen, G. O'Sullivan, V.K. Ivanov, A.N. Ipatov, J.T. Costello, and E. Kennedy, Phys. Rev. Lett. **78**, 3082 (1997).

[7] J.-M. Bizau *et al.*, Phys. Rev. Lett. **84**, 435 (2000).

[8] J.-M. Bizau *et al.*, Phys. Rev. Lett. **87**, 273002 (2001).

[9] A. Müller *et al.*, J. Phys. B **35**, L137 (2002).

[10] J.B. West, T. Andersen, R.L. Brooks, F. Folkmann, H. Kjeldsen, and H. Knudsen, Phys. Rev. A **63**, 052719 (2001).

[11] H. Kjeldsen, J.B. West, F. Folkmann, H. Knudsen, and T. Andersen, J. Phys. B **33**, 1403 (2000).

[12] K. Schulz, G. Kaindl, J.D. Bozek, P.A. Heimann, and A.S. Schlachter, J. Electron Spectrosc. Relat. Phenom. **79**, 253 (1996).

[13] P.A. Heimann *et al.*, Nucl. Instrum. Methods Phys. Res. A **319**, 106 (1992).

[14] A.M. Covington *et al.*, Phys. Rev. Lett. **87**, 243002 (2001); Phys. Rev. A **66**, 062710 (2002); for a pdf file of the ion-photon beam layout, see http://www-als.lbl.gov/als/quickguide/bl10.0.1.html

[15] C. Froese Fischer, T. Brage, and P. Jönsson, *Computational Atomic Structure—an MCHF Approach* (Institute of Physics, University of Reading, Berkshire, 1997).

[16] J-M. Esteva and G. Mehlman, Astrophys. J. **193**, 747 (1974).

[17] G. Mehlman, A.W. Weiss, and J.M. Esteva, Astrophys. J. **209**, 640 (1976).

[18] J. Brilly, E.T. Kennedy, and J-P. Mosnier, J. Phys. B **21**, 3685 (1988).